A case study integrating remote sensing and distinct element analysis to quarry slope stability assessment in the Monte Altissimo area, Italy

Authors: M. Francioni [a], R. Salvini [b],D. Stead [a], S. Litrico[b]

[a] Department of Earth Sciences, Simon Fraser University, Burnaby, BC, Canada

[b] Department of Environment, Earth and Physical Sciences and Centre of Geotechnologies, University of Siena, San Giovanni Valdarno, AR, Italy.

Corresponding author: M. Francioni, Department of Earth Sciences, Simon Fraser University, 8888 University Drive, Burnaby, B.C., Canada, V5A 1S6.

Phone: 778-782-7288. E-mail: mfrancio@sfu.ca. Phone: +1 778-782-7288.

Abstract

Over last decade geomatic techniques have been increasingly used for the geometrical characterization of rock slopes. Terrestrial laser scanning and digital terrestrial photogrammetry in particular are now frequently used in the characterization of joint surfaces and slope geometry. Although the use of these techniques for the structural characterization of slopes is widely documented, limited research has been undertaken to improve our understanding of the importance of the derived data quality in the construction of slope geometry imported into 3D numerical models. One of the most common problems encountered in the use of these techniques, especially in case of slopes with complex geometry, is the presence of occlusions. In this context, the aims of this paper are to describe how the integrated use of terrestrial laser scanning, digital terrestrial photogrammetry and topographic surveys can mitigate the influence of occlusions and how the slope geometry gained from these surveys can be important in slope stability analyses. For this purpose a case study in the Monte Altissimo area (Apuan Alps, Italy) will be presented. Several geomatic techniques were used for

studying a slope overhanging the Granolesa quarry. Special emphasis will be given to the importance of using Total Station and Differential GPS surveys as tools for data fusion. Moreover, in order to validate this procedure, the accuracy and precision of the output were determined through comparison of 3D models derived from laser scanning and digital terrestrial photogrammetry.
Furthermore, two different analyses with the three-dimensional distinct element code, 3DEC, were carried out in order to highlight the advantages and limitations of using data obtained from terrestrial remote sensing techniques as opposed to models based on topographic maps.

Key words: terrestrial laser scanning; digital terrestrial photogrammetry; intersection method; rock slope stability; 3D-distinct element models.

Introduction

Terrestrial Laser Scanning (TLS) and Digital Terrestrial Photogrammetry (DTP) are being increasingly used in the study of rock slopes (Feng and Röshoff, 2004; Abellán et al., 2006; Coggan et al., 2007; Tonon and Kottenstette, 2007; Jaboyedoff et al., 2008; Ferrero et al., 2009; Lato et al., 2009; Sturzenegger and Stead, 2009a and b; Salvini et al., 2011 and 2013). Using these techniques, it is possible to obtain very detailed information on the structural setting and slope geometry, even in the case of inaccessible steep slopes.

From past experience we note that there are two main aspects to consider during surveys with DTP and TLS:

- the distance between the camera/scanner and the slope
- the line-of-sight

Regarding DTP, depending on the camera-slope distance, different survey techniques can be chosen in order to work at an optimum scale. The scale (S), in photogrammetry, can be calculated using the following equation:

$S_{avg} = f/D$ (Equation 1)

where *f* is the focal length and D the distance. It is evident that, to achieve an optimum scale and ensure recognition of the geological features in the slope, it is necessary either to use a high focal length or to decrease the distance between the camera and the slope. Examples of these two techniques are documented by Sturzenegger and Stead (2009b), who obtained good results using high focal lengths (up to f = 400 mm). Vallet et al. (2000), Haarbrink and Eisenbeiss, (2008) and Salvini et al. (2011 and 2013), demonstrated the use of aerial vehicles to decrease the range between camera and slope. The use of an optimum photos scale in DTP is important because it influences the quality of the photogrammetric model. In this research the structural setting of the slope was studied through the use of stereo-pairs and manual stereo-restitution of features (fractures attitude, persistence and spacing). It is evident that the larger the scale of the photographs the more accurate will be the interpretation of geological features.

In TLS, the scanner-slope distance controls the resolution of the output (point cloud). If the laser scanner is set up close to the slope it is possible to obtain a very high resolution point cloud. In the case of a slope with complex geometry however, it may be necessary to acquire several point clouds from different scanner positions. However, it must be noted that the new generation of laser scanner tends to reduce the problem of scanner/slope distance making this technique even more attractive. In fact such scanners can reach long range and still maintain high resolution during data acquisition. As for the DTP, TLS point clouds were used to identify geological features. This step is discussed in detail in sections 3 and 4 and was performed by selecting points in the TLS model which represent the surface under study. It is clear that attaining a point cloud with a high resolution makes the measurement of features easier and more precise (Ferrero et al. 2009).

With regard to the line-of-sight, this parameter is important for both DTP and TLS as it controls the number of occlusions in the output point cloud data. Indeed, it is possible to use different lines-of-sight to obtain photographs and point clouds from different perspectives and thereby decrease the number of occlusions. The problem with this approach is that we obtain several point clouds and several photographs that need to be registered in the same reference system. Considering that the final accuracy of a 3D model is related to the quality of the images and the point cloud registration process, it follows that the use of a robust methodology for this process forms an essential prerequisite. In this context, one of the objectives of this paper is to show how the combined use of DTP and TLS, with Differential GPS (DGPS) and Total Station (TS), can be used to overcome the problem of occlusions and to register the data in a unique reference system. The survey's methodology presented in this research make it possible to set up several TLD and DTP stations (with different lines-of-sight) and to refer all the data to the same reference system. Such "non-static remote sensing surveys" allow overcoming of problems due to occlusions and slope orientation that generally occur using static surveys (Sturzenegger and Stead, 2009a and b; Lato et al., 2010).

The quality of point clouds and photograph registration is verified through the comparison of joint attitude measurements obtained from point clouds, stereoscopic models and compass techniques. The difference in the accuracy and precision of measurements from DTP and TLS are then discussed. Data obtained from these techniques can be used for different purposes. In this research the use of these data for the analysis of the rock slope stability using 3D numerical methods is presented. To understand the advantages and limitations of these techniques in the investigation of rock slope stability, a further analysis was undertaken using a 3D model derived from a topographic map at a scale of 1:1,000 and the results of the two different analyses compared and discussed.

2. Apuan Alps test site

In this paper, the case study of Granolesa quarry is presented. The quarry is located at the foot of Monte Altissimo, a mountain in the Carrara Marble District (Apuan Alps - Italy) (Fig. 1).

Marble extraction is one of the most important economic resources in the area. Extraction operations have a long history dating back to the Roman Empire. In fact, ancient gravestones made of Carrara Marble, have been recently discovered and attributed to the VI – II B.C. Extraction continued throughout the Roman Empire and is well documented in several archaeological excavations and reports. Mining increased further after the advent of blasting (XVIII century) and the improvement of infrastructure. Over the last 40 years blasting has been replaced by new techniques of excavation including the use of diamond wire and diamond saw blade which has decreased the degree of excavation-induced fragmentation. Nowadays, the Carrara district is the most important marble mining area in Europe with more than 100 active quarries and a production of around 1,000,000 tons/year of blocks and aggregated gravel (Carmignani et al., 2007).

Regarding the geology, the Apuan Alps belong to the Northern Apennines and are a compressional fold-thrust belt formed during the Oligocene due to the collision between the Corsica-Sardinia microplate and the Italian peninsula (Alvarez et al., 1974; Kligfield, 1979; Carmignani and Kligfield, 1990).

The stratigraphy consists of two non-metamorphic units (Tuscan Nappe and Liguride units) and a metamorphic complex. The latter is made up of two tectonic-metamorphic units, the ”Autoctono” and the overlaying “Unità di Massa”. The geometry of this complex is the result of two main tectonic-metamorphic events named D1 (late Oligocene-very early Miocene) and D2 (commencing in the early Miocene). During D1, there was deposition of non-metamorphic units (following the North-East direction) and compression caused by the under-thrust of the Adriatic plate. In these conditions, limestone, dated 180 My, was transformed to marble. Related to this event, is the formation of the metamorphic foliation (S1) that represents the axial plane of sheath folds which characterize the major part of the Apuan Alps. The folds range from microscopic to kilometre scale and the axes are generally oriented from North–West to South–East. During the subsequent D2 phase, all the structures developed in the D1 were re-folded again in a complex anti-formal stack geometry with the presence of parasitic folds. The D2 folding process is the likely cause of the exhumation of the metamorphic complex generated during the phase D1. Subsequently during the last stages of the D2 phase, brittle rather than ductile tectonics took place represented by open and kink folds and normal extension faults with a low and high angle. This extensional phase caused stretching, denudation and uplift phenomena, bringing higher and lower structures to the same level. Therefore, the Apuan Alps represent a wide tectonic window within the thickened Apennine Nappe (Carmignani and Kligfield, 1990).

3. Geomatic surveys

As mentioned above, the Carrara marble district represents a very important economic resource in Italy. Around 1,000 people currently work in the extraction industry in this region. For that reason, the use of innovative technologies for the study of rock slopes, open pits and underground quarries has become very important to improve safety in work places. In this context, this research shows the use of different geomatic techniques for the analysis of the Granolesa quarry and the overhanging rock slope.

3.1 Digital terrestrial photogrammetry

Digital Terrestrial Photogrammetry (DTP) is used in different fields, such as topographic mapping, architecture, engineering, and, more recently, environmental geology (Lemy and Hadjigeorgiou, 2003; Poropat 2003; Roncella et al., 2005; Redfern et al., 2007).

This is a remote sensing technique in which geometric properties of objects are determined by measurements of photographic images. For further details about the theory of this technique reference should be made to Slama (1980), Linder (2003) and Kraus (2007). In this work this technique, together with TLS, is used to collect the geometrical parameters necessary to understand the structural setting and carry out the stability analysis of the rock slope.

The authors have previously discussed the use of different methods for the photogrammetric acquisition depending on the slope morphology and the accessibility of rock faces (Sturzenegger and Stead, 2009b, Firpo et al., 2011). In this case, considering the elevation and the complex geometry of the slope (Fig. 1), an aerostatic helium inflated polyurethane balloon was used (Fig 2A).

Four electrical winches connected to dyneema cables, pulled the balloon from the ground and enabled the remote control of height and attitude. The equipment consisted of an aluminium frame, supporting two Nikon™ D80 digital cameras at its extremities (Fig 2B). The physical CCD frame size of the cameras was 2.36 x 1.58 cm with 10.2 million effective pixels.

Nikkor autofocus 2.8D lenses were used with a fixed focal length equal to f = 20 mm and a coverage angle of 70 degrees. Based on the sensor format, horizontal and vertical fields of view varied with the distance from the outcrops while the image size is represented in Table 1. Image acquisition was controlled by a PC-driven radio system which ensured both synchronous acquisition and correct setting of the camera shot angle in relation to the North. This function avoided problems relating to the yaw angle by maintaining right angles between the frame and the slope. A specifically-designed software package called Dragonfly (Menci Software s.r.l.) was used for this procedure. Therefore, the balloon ascended to the maximum desired height and during image acquisition remained completely stable. Furthermore, up-and-down movements of the photogrammetric equipment were controlled by pulleys so that the stereo-pairs were taken at various altitudes for each strip. Complete photographic acquisition was achieved covering the area by four vertical strips with about six stereo-pairs each. In order to avoid occlusions, these strips were acquired with different lines-of-sight (Table 2). Figure 2C shows the extent of the vertical strips adopted to cover the whole area while Figure 2D illustrates the direction of the aluminium frame during every acquisition (these directions are orthogonal to the line-of-sight).

The absolute orientation of the photographs was performed using the LPS module of ERDAS™ IMAGINE software. With the aim to obtain very precise output, 71 natural Ground Control Points (GCP) were measured using a Leica™ TCRP 1203+R1000 reflectorless Total Station (TS). The topographic survey will be discussed in-depth in paragraph 3.3. The Root Mean Square Error (RMSE) in image units (pixel) obtained for each strip during the absolute orientation process is shown in Table 2. As discussed previously the photogrammetric image scale depends on focal length and camera-slope distance. Considering the geometry of the slope and the fact that the acquisition with the aerostatic balloon proceeded vertically with fixed focal length, the scale changed in relation to the different zones of the slope. In the lowest area, where the camera-slope distance was closer, the scale was approximately 1:180 whereas, at the top of the slope it was around 1:300. Based on the data in Tables 1 and 2, and on the scale of the photogrammetric images (similar in every strip), it was possible to calculate the RMSE in ground units (cm). The results of this calculation are also shown in Table 2.

3.2 Terrestrial laser scanning

Terrestrial Laser Scanning (TLS) is an innovative survey technique for rapidly obtaining the geometry of slopes at high precision. Several types of laser scanner currently exist with different measurement principles and technical specification (Beraldin, 2004; Fröhlich and Mettenleiter, 2004). In this paper, a Leica™ ScanStation2 laser scanner was used for the survey. This instrument uses the time-of-flight technology to determine distances to an object and can scan to a distance of about 300 m. Nine point clouds were acquired to avoid occlusions in the output data (Fig. 3) and their resolution was set to 2 cm at a distance of 100 m. Considering the proximity between the laser scanner and the slope during the surveys a slope resolution of around 1 cm was achieved.

One of the most difficult steps in using TLS is the registration of point clouds. This process allows for the integration of several point clouds into a unique reference system. To overcome this problem, 49

High-Definition Surveying (HDS) targets were used during the data acquisition. These targets are automatically recognized by Leica™ Cyclone software (used for the TLS data post-processing) so that the registration can be easily computed by assigning them absolute coordinates. In addition, the TS was used to obtain very accurate measurements of the targets. This methodology and the registration process are discussed in-depth in the following section and in the discussion.

3.3 Total Station and intersection method

In this research use of a Total Station played a very important role allowing for the registration of photographs and point clouds in the same reference system.

A Total Station is an electronic/optical instrument used for topographic surveying which over recent has been increasingly used in mining surveying and civil engineering (Feng et al., 2001; Gan, 2011, Francioni et al., 2013). The Total Station represents an evolution of theodolite technology which through measurement of angles and distance and the use of trigonometry allows determination of the relative coordinates of surveyed points (X, Y and Z). To determine the absolute coordinates of a point (northing, easting and elevation), the TS must be set up at a known point and a reference direction for angle measurement (generally North) is required. The use of DGPS is necessary for both the measurement of TS origin and the calculation of the reference direction.

The TS, like other remote sensing techniques, has the problem of occlusion during the survey. In fact, to acquire the coordinate of a point, a direct line-of-sight must be established between the instrument and that point. When, a direct line-of-sight cannot be established, the instrument has to be set up in a new position. As discussed above, if the TS is moved to new locations, the positions of the instrument and the reference direction have to be calculated for each new station. In this paper, the Intersection Method (IM) was used to overcome this problem. IM is a technique for determining the position of the TS and the reference direction starting from at least two previously acquired known points (Fig. 4).

Calculation of the unknown point is based on trigonometry and, today, this can usually be automatically computed in the field if the TS is correctly set up. Using this technique and efficient work planning the DGPS only needs to be used at the first station (master).

In this research, the master was taken as station 1 (Figs. 3 and 5). From this station, several reference points were acquired so that a direct line-of-sight, with at least four of these points, was guaranteed for all the other planned stations (Fig. 3). Using this procedure, it was possible to set up the TS in nine different locations (Fig. 3 - the same station used for the TLS survey) and acquire the HDS targets and the natural GCPs within the same reference system. In total, the coordinates of 13 reference points used for IM, 71 GCPs for image orientation and 49 HDS targets for point cloud registration were acquired (Fig 5).

3.4 Differential GPS

In order to obtain the origin of the TS master station and establish the precise reference direction of the TS with respect to the North, a DGPS survey was performed using a Leica™ Viva GPS receiver (Fig. 5). The DGPS measurement was corrected by the use of Leica™ Geo Office software using data simultaneously recorded by the Lucca (LU) and Borgo a Mozzano (LU) permanent stations and the Root Mean Square Error (RMSE) achieved was equal to 2 cm. Due to the data post-processing, it was possible include in the same global reference system the coordinates of reference points for IM, HDS targets and natural GCPs.

4. Data processing and deliverables

The HDS targets and GCPs were referred to a unique system with a maximum IM error of 8 mm. From the absolute orientation of the photographs shown in Table 2, the stereoscopic models of the slope were derived and utilized for the stereo-restitution of geological features.

Based on the acquisition of the HDS targets, the registration of the nine point clouds in a one complete 3D model was possible with a mean error of about 5 mm.

Clearly, the construction of the 3D model provided data redundancy in some parts of the model. This problem was overcome by the use of a filter in Leica™ Cyclone software which allows for defining a minimum distance between two points. In so doing, the software removes the points that are closer than the specified range making possible the creation of a model with a reasonably constant resolution. In this case, a maximum resolution of 3 cm was chosen to allow easier and more precise extraction of geological features. The resolution was then decreased up to 30 cm during the creation of the 3DEC model. This was considered a good compromise to measure the complexities of the slope profile without building a too complex model geometry for use in the 3D numerical code. As the HDS targets and CGPs were in the same reference system, it was possible to merge the photogrammetric block with the TLS 3D model and obtain high resolution orthophotomosaics of the slope (Fig. 6).

As already documented by several authors (Krosley et al., 2006; Coggan et al., 2007; Sturzenegger and Stead, 2009a and b; Firpo et al., 2011; and Salvini et al., 2013) geological features such as block size and shape, and joint attitude and persistence can be restituted from DTP and TLS models.

In the stereoscopic model, surfaces restituted by the Stereo Analyst module of ERDAS™ IMAGINE were represented by triangles drawn co-planar with the discontinuities (Figs. 7A and B). Their dip and dip direction were calculated using spatial analysis techniques with Esri™ ArcInfo Workstation software. In fact, using this workstation it was possible to perform a GIS analysis which defined the joint attitudes through the calculation of “Aspect” (dip direction) and the “Slope” (dip) of each triangular surface.

It must be highlighted that manual stereo-restitution of feature, although providing a high level of data interpretability during the stereo-restitution, is prone to human error.

In contrast, on the point cloud, the attitude of the surfaces was obtained by Leica™ Cyclone using a semi-automatic procedure. In practice, several points (at least three) representing the surface under investigation were selected on the point cloud, and the software then automatically recreated that surface (Fig. 7C). The algorithm used for this procedure is a best-fit algorithm developed by Leica Geosystems. The spatial vector components u_x, u_y and u_z were obtained from this surface and, through the use of Equations 2 and 3, it was possible to calculate the dip direction and dip respectively:

Dip direction = $arctan\ (u_x/u_y) + \theta$ (Equation 2)

where:

$\theta = 0°$ for $u_x \geq 0$ and $u_y \geq 0$

$\theta = 360°$ for $u_x \leq 0$ and $u_y \geq 0$

$\theta = 360°$ in all the other cases

and

Dip = $\arctan\ [u_z/(u_x^2 + u_x^2)^{-1}]$ (Equation 3)

In this study, a validation procedure was followed in order to assess the accuracy of the joint attitudes extrapolated from TLS and DTP models. The measurements from the two proposed geospatial methodologies were compared with data from traditional engineering geological compass surveys. Eight surfaces were chosen at the quarry face for this purpose and, to avoid affecting the results with a single error during the measurement, every surface was drawn ten times and the mean value used for the comparison.

Table 3 shows the results of this validation procedure with the mean attitude values determined from the compass, DTP and TLS measurements. Moreover, the box plot representation in Figure 8 highlights the variation in degrees between compass and remote sensing measurements (differences represented in absolute values). The high accuracy and precision of the TLS and DTP is evident from this box plot where mean values are similar to the compass measurements and the standard deviation is always less than 10 degrees. Nevertheless, the graph also highlights the higher precision of the measurements carried out on the TLS model. This is mainly due to the very high resolution of the point clouds (around 1 cm of resolution on the slope) and to the methodology used for the extraction of the dip and dip direction. In fact, as discussed above, the procedure used for the attitude determination for the surfaces in the TLS model is semi-automatic and reduces human error during the surface extrapolation. In contrast, the surfaces on the stereoscopic model were drawn manually so that the precision of the measurements is related to the experience and skill of the drawer and tend to be less precise.

It is important however to considerer the flexibility of the DTP when comparing it to TLS. In fact, even in the worst case scenario when the dip direction of fractures is orthogonal to the line-of-sight, it is possible from the stereoscopic model to interpret of their attitude. In contrast, this can be very difficult using the model derived from TLS, especially when the resolution of point clouds is lower than the fracture aperture.

Data from the engineering geological survey, DTP and TLS were all subsequently integrated to define the structural setting of the slope. The attitudes of more than 500 joint surfaces were measured using the three surveying techniques. Joint persistence and spacing were measured in the field and on the stereoscopic model by 3D linear representation whereas the aperture, Joint Compressive Strength (JCS - Deere and Miller, 1966) and Joint Roughness Coefficient (JRC - Barton, 1973) were obtained only from the engineering geological survey. Table 4 shows the results gained from this study.

5. Remote sensing data and 3D Distinct Element Code for the stability analysis of the slope

We have previously illustrated how it is possible to use remote sensing techniques for the geometrical and structural characterization of rock slopes. This information was used in the stability analysis of the rock slope with the three dimensional distinct element code, 3DEC, (Itasca™, 2008). This code uses an explicit time-stepping scheme to solve the Newton's equation of motion and it treats the rock mass as a discontinuum material where the joints are the main control in the analysis of the rock mass. The discontinuities cut the rock mass in blocks which can be assigned rigid or deformable stress–strain constitutive criteria depending on the rock mass characteristics. Different constitutive criteria can also be assigned to the discontinuities which are treated as boundary conditions along which large displacements and rotations are permitted. Cundall (1988), Hart et al. (1988) and Itasca™ (2012) describe the principles of distinct element code and 3DEC in more detail. This software has been used by several authors recently in both case studies and conceptual models (Yeung and Wong, 2007; Brideau and Stead, 2010; Kalenchuk, 2010; Brideau and Stead, 2011 and 2012; Firpo et al., 2011). In order to make the data amenable for incorporation into 3DEC pre-processing procedure is required which is described below. Moreover, to understand the advantages and limitations of using terrestrial remote sensing techniques for the investigation of slopes, two different 3DEC analyses will be presented; the first using a 3D model derived from TLS and, the second, derived from a topographic map with a scale of 1:1,000. The choice of using the TLS point cloud rather than the eventual DTP point cloud derived from image matching algorithms and manual stereo-restitution, was based on several reasons. Although software with image matching algorithms has allowed very high precision in the construction of 3D models in the last decade, the results of the calculations are strictly related to the quality of the photographs. Therefore, the complexity of the slope geometry, experience in the use of aerostatic balloons, the results of the comparison between TLS and DTP and the actual availability of a very precise TLS model have all led the authors to use the latter for the provision of data for analysis using the 3DEC code.

5.1 Creation of the slope geometry in 3DEC

The Rhinoceros™ SR[4] (CAD suite developed by McNeel and Associates, 2011) was used to manage the TLS point clouds and create both the 3D model (Fig. 9A) and triangulated mesh. As mentioned in the previous section, the TLS point cloud was resampled before importing into the 3DEC model. A resolution of 30 cm was retained and considered sufficient by the authors to include all the relevant scale geometrical variations in the slope (Fig. 9A). The mesh obtained from this model was then exported and made compatible with 3DEC using the Itasca™ software, Kubrix (Fig. 9B).

Using this software, it was possible to create a 3DEC model closely approximating the true geometry of the slope. The structural setting of the slope could have been defined in 3DEC using the data presented in Tables 3 and 4. In this case, however, the purpose of the analysis was to highlight the advantages of using a model created from geomatic techniques. Moreover, the joint geometry achieved from the above mentioned surveys, represents the situation on the slope face but it is suggested that this may rarely be fully representative of the actual situation at depth inside the slope. Therefore the authors in these preliminary models decided to use a joint spacing three time wider than the measured value (1.1 m for K1, 2.3 m for K2 and 7.9 m for K3).This enabled practical computer runtimes without changing the relative spacing between joints and compromising the objectives of the research.

In order to understand the advantages and limitations of using terrestrial remote sensing techniques, a further 3DEC analysis was carried out using the slope geometry obtained from the topographic map at a scale of 1:1,000 (Figs 9C and D). The procedure used to create this additional 3DEC model was similar to that outlined for the TLS data.

5.2 3DEC analysis

As discussed above, the geometric models created from TLS and the topographic map were used for the 3DEC analyses. In order not to introduce increased uncertainty in the calculation and to focus the study on the role of measured slope geometry on slope deformation, the same typical joint properties were assumed for all the joint sets. Three simulations were carried out for both models using different joints properties with the aim to investigate the models susceptibility to instability (Table 5).

Considering that the entire slope comprises marble with very high strength properties and that the principal focus of this research was to analyse the role of different slope geometries with respect to joint behaviour, the rock mass blocks were assumed to be rigid (non-deformable with a density equal to 2,700 Kg/m^3).

A comparison of the response of the two models was undertaken using the Shear Strength Reduction Factor (SRF – Dawson and Roth, 1999; Griffiths and Lane, 1999) where the shear strengths of all the component materials were iteratively decreased until the slope failed. Clearly, considering that the rock mass material was assumed to be rigid, the SRF was applied only to the joint properties. The results of this comparison are shown in Table 6 and Figure 10 where it is possible to see how, in the TLS model, the SRF is consistently lower than in the topographic model.

As all the input parameters used in the 3DEC analyses were the same for both models, it is evident that the differences in the SRF were due to the geometry. In fact, although the topographic map at a scale of 1:1,000 may be a reliable representation of morphology it is unable to represent some slope peculiarities such as the overhanging geometry present in this case-study. Therefore, the 3D model achieved may not always be fully representative of the actual localized slope geometry. Figure 11 highlights the differences between the geometry extracted from the topographic map and the TLS. Figures 11A and B show the 3D model from the topographic map and a 2D section through it respectively whereas Figures 11 C and D show the same for the TLS model.

The slope in the first two images (Fig 11 A and B) is fairly regular with a steep slope while, in the images in Fig 11 C and D, it is characterized by a more complex morphology with an overhanging geometry.

This difference in the local slope morphology is most probably the cause of the SRF differences obtained in the analyses. In fact, this overhanging rock mass has a volume of about 14 m^3 (calculated in Rhinoceros - McNeel and Associates, 2011) which is not evident from the topographic model. Clearly, the overhanging rock volume can influence the results of stability analysis and consequently the SRF due to the necessity to consider the existence of a key block and block theory (Goodman and Shi, 1985).

6. Discussion

This paper evaluates the importance of the integrated use of topographic and remote sensing techniques in slope stability analysis. The methodology described attempts to overcome a frequent problem related to the accuracy and completeness of data representing the rock slope morphology. Special emphasis is given to the use of IM as a tool for data integration and the role that different geometric models can have in the results of 3D slope stability analyses.

With regard to the photogrammetric survey, the authors show how the use of an aerostatic balloon in the investigation of the quarry and the overhanging slope is able to overcome problems related to the slope height and the complex geometry of the rock slope face. Table 2 shows the errors obtained during the orientation process; these are considered acceptable in view of the complexity of the survey. Although the use of the aerostatic balloon was important to avoid hidden zones, the use of this tool for the photogrammetric survey tends to be complicated. In fact, the instrumentation needs to be set up over a large area at the foot of the slope and the maximum height that can be achieved is about 300 m. Moreover, the wind and the cost of the helium can represent additional limitations in the use of this tool. The advent of new technologies, like Unmanned Aerial Vehicles (UAV) (Haarbrink and Eisenbeiss, 2008; Niethammer et al., 2010; Tahar et al., 2012; Danzi et al., 2013; Salvini et al., 2014) and the development of new photogrammetric survey techniques including the use of long range focal length (Sturzenegger and Stead, 2009b), can overcome these problems making DTP even more attractive and easy to use.

Regarding the TLS, it was used to obtain a very high resolution 3D model and to define a new approach for the point cloud registration. Several scans were acquired using different lines-of-sight to avoid occlusions at the rock slope face and the IM was used to join the point clouds into a unique model.

IM played an important role in this research as it allowed for measuring a large number of GCPs and HDS targets in the same reference system. In so doing it was possible to acquire photographs (DTP) and point clouds (TLS) using different lines-of-sight and to combine all the data into the same reference system.

Using this “non-static survey” methodology it was possible to overcome commonly reported problems associates with the use of DTP and TLS. As discussed by several authors (Sturzenegger and Stead, 2009a and b; Ferrero et al., 2010; Lato et al. 2010), the use of remote sensing techniques can lead to problems related to slope orientation and differences in the point cloud density. Ferrero et al., 2010 described the use of a new software code to determine of the rock discontinuities by means of the application of a segmentation algorithm. They highlight the advantage of using this new approach and how the accuracy of derived data always increases with a higher point density. Sturzenegger and Stead (2009 a and b) and Lato et al. (2010) highlight the importance of the line-of-sight in the use of DTP and TLS and how the use of “static TLS surveys” leads to problems related to the slope orientation. In these situations, Lato et al. (2010) suggested the use of mathematical correction to overcome these problems or, when possible, the use of multiple TLS stations.

The quality of the DTP and TLS output (gained with this “non-static TLS survey)’ was validated by comparison of measurements undertaken on the same structures on both models. Measurements showed a maximum variance of 8° and 3° for the DTP and TLS respectively compared with the attitude obtained using a conventional engineering compass. This result agrees with previous comparative studies carried out by Coggan et al., (2007). The DTP variance may partially be due to the error in the absolute orientation of the images (Table 2) but, is considered primarily to be the result of possible human error during the stereo-restitution of the 3D features. Different photogrammetric techniques (Kemeny and Post, 2003; Roncella et al., 2005) and software (e.g. 3DM Analyst software – Adam Technology 2012) can overcome this problem creating a very accurate 3D model from the photogrammetric block, where it is possible to use the same joint extrapolation technique as used in the TLS model. Sturzenegger and Stead (2009b) showed that with careful orientation the attitude of discontinuities extracted from the photogrammetric model can have a similar accuracy to that obtained from TLS.

However, in this paper the results achieved from the validation process confirmed the good quality of the data that was used to define the geometry and the structural setting of the slope, and were used to analyse the stability with 3DEC. With the principal aim of highlighting the advantages and limitations of using terrestrial remote sensing data, two different slope models were analysed with the 3DEC code. The first was obtained from the topographic map and the second from TLS. The same rock mass and joint properties were assumed in both models and three different analyses were done with decreasing joint properties (Table 5). The reduction of joint properties caused a decrease in the SRF (Table 6). Moreover, careful examination of the graph in Figure 10 shows important differences in the behaviour between the TLS and topographic model. In fact, in the three analyses carried out, the TLS model consistently has a lower SRF and, in the third analysis, the SRF falls to below 1. As mentioned previously this behaviour is related to the different geometry of the models and, in particular, to the overhanging geometry that characterizes the top of the quarry in the TLS model.

A clear example is illustrated in the Figure 11 where it is possible to see the difference in the two analyses in terms of the sliding process. The morphological profile represented in Figure 11B shows how the hypothetical failure resembles either a planar or wedge type mechanism whereas, in Figure 11D, rock fall may be indicated. It must be emphasized that a similar overhanging morphology is not evident from the 2D topographic map.

Considering the limitations of the proposed methodology, it should be noted that the data processing/interpretation time when dealing with accurate and detailed data are longer and the model construction more complex.

Such detailed slope geometry is useful in complex morphologies but may be unnecessary in simple slopes where an high scale topographic map can be suitable.

Another aspect to take into account is that, in the 3DEC analyses, a point of origin is needed to define the joint sets and this can play a very important role in terms of key block analysis and, consequently, SRF. It is evident that the effect of this variation is strictly dependent on the geometry of the slope and joint sets. In this case study, since the thickness of the overhanging part of the slope varies from 3 to 5 meters (calculated in Rhinoceros - McNeel and Associates, 2011), it will always be wider than the spacing of the joint systems that daylight on the slope (K1 and K2). It follows that a variation of the seed point will change the volume of the failing blocks and the SRF but will not modify the kinematics and general results. Using a different seed point, the analysis with a TLS model will always show a different failure mechanism and a lower SRF than that using the topographic model.

The main joint sets used in the analysis were obtained from a statistical study (with an increased bedding spacing adopted to allow practical simulation times). This approach although reasonable for a probabilistic slope stability study does not represent the real situation in the slope with respect to the observed presence of discrete fractures and the influence of brittle fracturing due to blasting or excavation. Remote sensing techniques can be useful for the definition of brittle fracturing but only the rock slope face can be characterized by the use of these techniques. For that reason, a statistical analysis will be always required to generate discontinuities behind the observed rock face. The use of a stochastic discrete fracture network (DFN) model can be important to optimize the use of discontinuity data from conventional field surveys, remote sensing techniques and boreholes. In fact, in DFN modelling, it is possible define for each discontinuity set the orientation, persistence and spatial location. Several authors have shown the potential of a DFN approach for creating realistic geometric models that reflect the heterogeneity of fractured rock mass (Elmo, 2006; Pine et al., 2006; Elmo and Stead, 2010). Nevertheless, it must be considered that trace length and discontinuity shape can only be approximated and the discontinuities shape presumed; as a result, this can lead to significant uncertainty in the DFN model and related block size/shape distributions. Elmo et al. (2007), Rogers et al. (2007), Rogers et al. (2009) and Stead et al. (2009) have demonstrated how the block size distributions is strictly influenced by trace length, truncation bias and discontinuity intensity. Sturzenegger et al. (2011) have recently illustrated the generation of DFN models using discontinuity parameters measured from terrestrial remote sensing. They highlighted the advantages and limitations of using this approach and suggested guidelines for the correct use of remote sensing techniques as alternative tools for the generation of advanced numerical models for slope stability analysis methods such as FracMan rock wedge analysis, Elfen and Slope Model (e.g. Cundall and Damjanac, 2009; Elmo and Stead, 2010). An integrated approach using geomechanical models that combines observed and measured discontinuities with statistically generated fractured networks may provide the most efficient remote sensing approach for the near future. Clearly, there remains a need for improved understanding of the uncertainty associated with the remote sensing measurement of rock slopes and discontinuities. The use of these techniques, combined with geostatistics is critical potential for the improved understanding of rock slope failure mechanisms.

In this context several important questions must be answered in the future including to what practical scale we can measure joints in a rock slope, how important is the truncation of measured joints to block size estimation and the kinematic assessment of rock slope failure mechanisms and finally what level of data will it be feasible and more importantly practical to include in future geomechanical models.

7. Conclusion

In the present research, DTP and TLS are shown to provide powerful modelling and analytical tools in the study of the geometry of a rock slope. DTP was carried out through the use of an aerostatic balloon. This technique overcomes the problem of occlusions arising from the elevation (up to 300 m) and the complex geometry of the slope. TLS was performed using a short range laser scanner. A "non-static TLS survey" was carried out to avoid hidden zones and problems related to the slope orientation and point clouds density. This type of approach was possible thanks to the use of IM and provides an alternative methodology with which to overcome the biases that commonly affect remote sensing data.

Table 7 summarize the advantages and limitations of these remote sensing techniques based on the experience gained by the authors in this and previous researches (Sturzenegger and Stead; 2009a and b; Firpo et al, 2011; Francioni, 2013).

Slope geometry simulations using the 3D DEM 3DEC code were carried out with decreasing joint properties (Table 5) and with two different slope geometry models (one derived from the topographic map and the other from TLS). These simulations clearly demonstrate that the results of the stability analysis in terms of the shear strength reduction factor, are influenced significantly by the measured geometry (Table 6). This phenomenon shows that subtle variations in the slope geometry can change the simulated failure mechanism and consequently the results obtained using key block theory. Based on our results, Table 8 summarizes the improvements that remote sensing techniques can produce in the analysis of slopes with 3D distinct element codes. This is a modified classification based on Stead et al., (2006) and considers the critical input parameters in distinct element methods and, based on Francioni (2013) and this study, the potential role of remote sensing techniques in the analyses of slopes.

Finally, it is emphasised that this research represents an initial step in understanding the importance of slopes geometry detail in the analyses conducted using advanced three-dimensional geomechanical codes and the role that remote sensing techniques offer in acquiring improved geometrical slope details. As discussed in the previous section, further studies are needed to investigate the influence of parameters assumed in the mechanical model. Moreover the results gained from this research are related to the geometry of the slope under study and should be investigated further for varied slope geometry case studies and failure mechanisms. A detailed slope geometry is may be useful in complex morphologies but could be unnecessary in simple slopes where a high scale topographic map can be suitable and can decrease the processing/interpretation time of the analyses. Each individual slope must be considered with respect to the potential importance of complex slope geometrical variations and assessed in relation to the geological structure and preliminary kinematic considerations.

Acknowledgments

The authors wish to thank the Tuscany Region which funded this research (Announcement 6744/2008 POR CREO 2007-2013). Moreover, we are extremely grateful to Henraux S.p.A., Prof. Pier Lorenzo Fantozzi (University of Siena), Geol. Sergio Mancini, Geol. Vinicio Lorenzoni, Ing. Matteo Lapini (Ingeo Systems s.r.l.) for their assistance and advices in this research.

References

ADAM Technology, 2012. 3DM analyst 2.1, 3DM CalibCam 2.1. http://www.adamtech.com.au.

Abellán, A., Vilaplana, J.M., Martinez, J., 2006. Application of a long-range Terrestrial Laser Scanner to a detailed rock fall study at Vall de Núria (Eastern Pyrenees, Spain). Engineering Geology 88, 136-148.

Alvafez, W., Cocozza T., Wezel, F.C., 1974. Fragmentation of the Alpine orogenic belt by microplate dispersal. Nature 248, 309-314.

Barton, N.R., 1973. Review of a new shear strength criterion for rock joints. Engineering Geology 7, 287-332.

Beraldin, J. A., 2004. Integration of laser scanning and close-range photogrammetry— the last decade and beyond. Proceedings: XXth International Society for Photogrammetry and Remote Sensing (ISPRS) Congress, Istanbul, Turkey, 972-983.

Brideau, M. A., and Stead, D., 2012. Evaluating kinematic controls on planar translational slope failure mechanisms using three-dimensional distinct element modelling. Geotechnical and Geological Engineering, 30(4): 991-1011.

Brideau, M. A., and Stead, D., 2011. The influence of three-dimensional kinematic controls on rock slope stability. In: D. Sainsbury , R. Hart, C. Detournay, and M. Nelson (eds) Proceedings of the 2nd International FLAC/DEM Symposium, Melbourne, Australia, February 14-16 2011, pp. 213-220.

Brideau, M, A., Stead, D., 2010. Controls on block toppling Using a three-dimensional distinct element approach. Rock Mech Rock Eng 43, 241-260.

Carmignani, L.,Conti, P., Fantozzi, P.L., Mancini S., Massa G., Molli G., Vaselli L., 2007. I marmi delle Alpi Apuane. Geoitalia; 21, 19-30.

Carmignani, L., Kligfield, R., 1990. Crustal extension in the Northern Apennines: the transition from compression to extension in the Alpi Apuane core complex. Tectonics, v9,1275-1303.

Coggan, J.S., Wetherelt, A., Gwynn, X.P., Flynn, Z., 2007. Comparison of hand-mapping with remote data capture systems for effective rock mass characterisation, 11th Congress of International Society for Rock Mechanics, Lisbon 2007, 9th - 13th Jul 2007, Proceedings of 11th Congress of the International Society for Rock Mechanics - the second half century of rock mechanics, 1, 201-205.

Cundall, P.A., Damjanac, B., 2009. A comprehensive 3D model for rock slopes based on micromechanics. Slope Stability Symposium, Santiago, Chile, 9-11 November. 10 pp.

Cundall, P.A., 1988. Formulation of a three-dimensional distinct element model–part I. A scheme to detect and represent contacts in a system composed of many polyhedral blocks. Int J Rock Mech Min Sci Geomech Abstr 25 (3):107-116.

Danzi, M., Di Crescenzo, G., Ramondini, M., Santo, A., (2013). Use of unmanned aerial vehicles (UAVs) for photogrammetric surveys in rockfall instability studies. Rendiconti Online Societa Geologica Italiana, 24, 82-85.

Dawson, E.M., Roth, W.H., Drescher, A., 1999. Slope Stability Analysis by Strength Reduction, Geotechnique, 49(6), 835-840.

Deere, D.U., Miller, R.P., 1966. Engineering classification and index properties for intact rock. Technical Report AFNL-TR-65-116.Air Force Weapons Laboratory, New Mexico. 277 pp.

Elmo, D., 2006. Evaluation of a hybrid FEM/DEM approach for determination of rock mass strength using a combination of discontinuity mapping and fracture mechanics modelling, with particular emphasis on modelling of jointed pillars. Ph.D. thesis. Camborne School of Mines, University of Exeter, UK.

Elmo, D., Yan, M., Stead, D., Rogers, S., 2007. The importance of intact rock bridges in the stability of high rock slopes: a quantitative investigation using an integrated numerical modelling — discrete fracture network approach. Proceedings: International Symposium on Rock Slope Stability in Open Pit Mining and Civil Engineering, Perth 12-14 September, pp 253-266.

Elmo, D., Stead, D., 2010. An integrated numerical modelling–discrete fracture network approach applied to the characterisation of rock mass strength of naturally fractured pillars. Rock Mech Rock Eng 43, 3-19.

Fekete, S., Diederichs, M., Lato, M., 2010. Geotechnical and operational applications for 3-dimensional laser scanning in drill and blast tunnels. Tunnelling and Underground Space Technology, 25, 614-628.

Feng, Q.H., Röshoff, K., 2004. In-situ mapping and documentation of rock faces using a full-coverage 3D laser scanner technique. International Journal of Rock Mechanics and Mining Sciences 41 (3), 139-144.

Feng, Q., Sjögren, P., Stephansson, O., Jing, L., 2001. Measuring fracture orientation at exposed rock faces by using a non-reflector total station. Engineering Geology 59, 133-146.

Ferrero, M. Migliazza, R. Roncella, E. Rabbi (2010). Rock slopes risk assessment based on advanced techniques. Landslide 8, 221-231.

Ferrero, A. M., Forlani G., Rondella R., Voyat H.I., 2009. Advanced geostructural survey methods applied to rock mass characterization. Rock Mech Rock Eng 42 (4), 631-65.

Firpo, G., Salvini, R., Francioni, M., Ranjith, P.G., 2011. Use of Digital Terrestrial Photogrammetry in rocky slope stability analysis by Distinct Element Numerical Methods. International Journal of Rock Mechanics and Mining 48 (7), 1045-1054.

Francioni, M., 2013. Developments in the study of rock slopes: an integrated terrestrial remote sensing – stability analysis approach. PhD Thesis. University of Siena.

Francioni, M., Girgenti, C., Vanneschi, C., 2013. Underground quarrying industry and terrestrial laser scanning. Rendiconti Online Societa Geologica Italiana 24, 140-142.

Fröhlich, C., Mettenleiter, M., 2004. Terrestrial laser scanning — new perspectives in 3D surveying. In: Thies, M., Koch, B., Spiecker, H., Weinacker, H. (Eds.), Laser-scanners for Forest and Landscape Assessment. International Archives of Photogrammetry, Remote Sensing and Spatial Information Sciences, vol. XXXVI-8/W2, 7-13.

Gan, Z.R., 2011. Application of GTS-311 Total Station in a slope-shaft breakthrough on error analysis. Advanced Materials Research. 5839, 243-249.

Goodman, R., E., Shi G.H., 1985. Block theory and its application to rock engineering. Prentice Hall, New Jersey, 338 pp.

Griffiths, D.V., Lane, P.A., 1999. Slope Stability Analysis by Finite Elements, Geotechnique, 49(3), 387-403.

Hart, R., Cundall, P.A., Lemos J., 1988. Formulation of a three-dimensional distinct element model– part II. Mechanical calculations for motion and interaction of a system composed of many polyhedral blocks. Int J Rock Mech Min Sci Geomech Abstr 25 (3),117-125.

Haarbrink, R.B., Eisenbeiss, H., 2008. Accurate DSM production from unmanned helicopter systems. International Archives of Photogrammetry, Remote Sensing and Spatial Information Sciences, XXXVII/B1. PRC, Beijing, 159-164.

Itasca™, 2008. 3DEC version 4.10, Itasca Consulting Group Inc. Minneapolis, Minnesota. http://www.itascacg.com/3dec/.

Jaboyedoff, M., Oppikofer, T., Minoia, R., Locat, J., Turmel, D., 2008. Terrestrial LIDAR investigation of the 2004 rockslide along Petit Champlain Street, Québec City(Québec, Canada). Proceedings: 4th Canadian Conference on Geohazards, 20-24May, Québec, Canada, 8 pp.

Kalenchuk, K. S., 2010. Multi-Dimensional Analysis of Large, Complex Slope Instability. PhD Thesis. Queen's University.

Kemeny J., Post R. (2003): Estimating three-dimensional rock discontinuity orientation from digital images of fracture traces. Computers & Geosciences 29 (2003), pp. 65-77.

Kligfield, R., 1979. The Northern Apennines as a collisional orogeny. Am. J. Sci. 279, 676-69.

Kraus, K., 2007. Photogrammetry, Geometry from Images and Laser Scans. Berlin: De Gruyter.

Krosley, L.K., Shaffner, P.T., Oerter, E., Ortiz, T., 2006. Digital ground-based photogrammetry for measuring discontinuity orientations in steep rock exposures. Proceedings: 41st U.S. Symposium on Rock Mechanics (USRMS), Golden, Colorado, June 17-21, 13 pp.

Lato M, Diederichs M, and Hutchinson D.J (2010) "Bias correction for static LiDAR scanning of rock outcrops for structural characterization" Rock Mechanics and Rock Engineering, 43 (5), 615-628.

Lato, M., Diederichs, M.S., Hutchinson, D.J., Harrap, R., 2009. Optimization of LiDAR scanning and processing for automated structural evaluation of discontinuities in rock masses. International Journal of Rock Mechanics and Mining Sciences 46, 194-199.

Lemy, F., Hadjigeorgiou, J., 2003. Discontinuity trace map construction using photographs of rock exposures. Int J Rock Mech Min Sci 40 903-17.

Linder, W., 2003. Digital Photogrammetry - Theory and Applications. Heidelberg.

McNeel and Associates, 2011. Rhinoceros 4, SR9. http://www.rhino3d.com/download/rhino/4.0.

Niethammer, U., Rothmund S., James M. R., Travelletti J., Joswig M., 2010. UAV-based remote sensing of landslides. International Archives of Photogrammetry, Remote Sensing and Spatial Information Sciences, Vol. XXXVIII, 5.

Pine, R.J., Coggan, J.S., Flynn, Z.N., Elmo, D., 2006. The development of a new numerical modelling approach for naturally fractured rock masses. Rock Mech Rock Eng 39(5), 395-419.

Poropat, G., 2003. A new tool for mapping rock mass structure in open pits. CSIRO.

Redfern, J., Hodgetts, D., Fabuel-Perez, I., 2007. Digital analysis brings renaissance for petroleum geology outcrop studies in North Africa. First Break 25, 81-87.

Rogers, S.F., Kennard, D.K., Dershowitz, W.S., van As, A., 2007. Characterising the in situ fragmentation of a fractured rock mass using a discrete fracture network approach. Proceedings: 1st Canada–US Rock Mechanics Symposium, Vancouver, 27–31 May, pp. 101-106.

Rogers, S.F., Elmo, D., Beddoes, R., 2009. Mine scale DFN modelling and rapid upscaling in geomechanical simulations of large open pits. Rock slope characterization for large open pits and high mountain slopes. Proceedings: International Symposium on Rock Slope Stability in Open Pit Mining and Civil Engineering, Santiago, Chile, November 2009. 11 pp.

Roncella, R., Forlani, G., Remondino, F., 2005. Photogrammetry for geological applications: automatic retrieval of discontinuity orientation in rock slopes. In:Proc SPIE-IS&T electronic imaging, Videometrics 5665,17-27.

Salvini R., Riccucci S., Gullì D., Giovannini R., Vanneschi C., Francioni M., 2014. Geological application of UAV photogrammetry and terrestrial laser scanning in marble quarrying (Apuan Alps, Italy). Accepted to XII International Congress of IAEG (International Association for Engineering Geology and the Environment), Turin (Italy) September 15-19, 2014.

Salvini, R., Fantozzi, P.L., Francioni, M., Riccucci, S., Bonciani, F., Mancini, S., 2011. Stability analysis of "Grotta delle Felci" Cliff (Capri Island, Italy): structural, engineering–geological, photogrammetric surveys and laser scanning. B Eng Geol Environ 70, 549-557.

Salvini, R., Francioni, M., Riccucci, S., Bonciani, F., Callegari, I., 2013. Photogrammetry and laser scanning for analyzing slope stability and rock fall runout along the Domodossola–Iselle railway, the Italian Alps. Geomorphology 185, 110-122.

Slama, C.C. (Ed.), 1980. Manual of Photogrammetry, 4th edition. American Society of photogrammetry, Falls Church, 1056 pp.

Stead, D., Sturzenegger, M., Gao, F., Elmo, D., Eberhardt, E., 2009. Rock slope characterization for large open pits and high mountain slopes. Proceedings: International Symposium on Rock Slope Stability in Open Pit Mining and Civil Engineering, Santiago, Chile, November 2009, 15 pp.

Stead D., Eberhardt E., Coggan J.S., (2006). Developments in the characterization of complex rock slope deformation and failure using numerical modelling techniques. Engineering Geology 83 (2006) 217– 235.

Sturzenegger, M., Stead, D. and Elmo, E., 2011 Terrestrial remote sensing-based estimation of discontinuity frequency, mean trace length, block size/shape and dependence on observation scale. Engineering Geology,119:(3-4), 96-111.

Sturzenegger, M., Stead, D., 2009(a). Close-range terrestrial digital photogrammetry and terrestrial laser scanning for discontinuity characterization on rock cuts. Engineering Geology 106, 163-182.

Sturzenegger, M., Stead, D., 2009(b). Quantifying discontinuity orientation and persistence on high mountain rock slopes and large landslides using terrestrial remote sensing techniques. Natural Hazards and Earth System Sciences 9 (2), 267-287.

Tahar, K.N., Ahmad, A., Akib, W.A.A.W.M., Mohdl, W.M.N.W., 2012. A new approach on production of slope map using autonomous Unmanned aerial vehicle. International Journal of Physical Sciences Vol. 7(42), 5678-5686.

Tatone, B.S.A., Grasselli, G., 2010. An Investigation of Discontinuity Roughness Scale Dependency Using High-Resolution Surface Measurements. Rock Mechanics and Rock Engineering. July 2013, Volume 46, Issue 4, pp 657-681.

Tonon, F., Kottenstette, J.T., 2007. Laser and photogrammetric methods for rock face characterization. Report on a Workshop Held in Golden, Colorado, June 17-18, 2006. American Rock Mechanics Association, 6 pp.

Tuckey, Z., Stead, D., Eberhardt, E. 2013. An Integrated Approach for Understanding Uncertainty of Discontinuity Persistence and Intact Rock Bridges in Large Open Pit Slopes,Slope Stability 2013, Brisbane, Sept 2013, (In press).

Vallet, J., Skaloud, J., Kölbl, O., Merminod, B., 2000. Development of a helicopter based integrated system for avalanche and hazard management. International Archives of Photogrammetry and Remote Sensing 33 (B2), 565-572.

Yeung M.R., Wong K.L., 2007. Three-dimensional kinematic conditions for toppling. In: Eberhardt E, Stead D, Morrison T (eds) 1st Canada-US rock mechanics symposium. Balkema, Rotterdam, pp 335-340.

Figures:

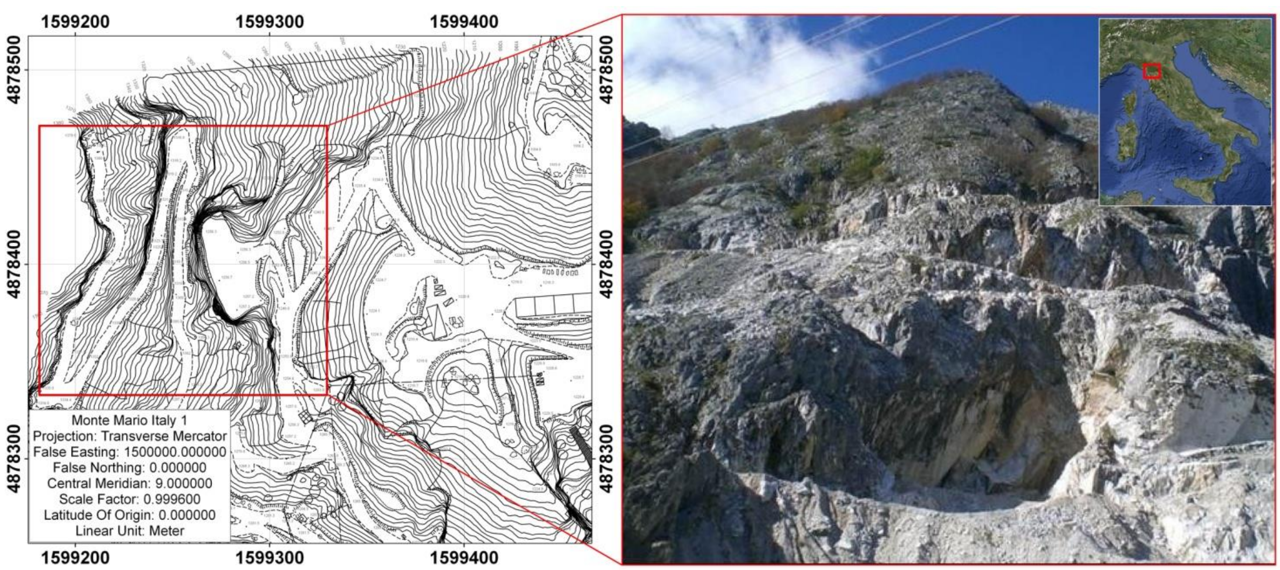

Fig. 1. The Granolesa quarry. The photograph on the right shows the view of rock slope from the East to the North.

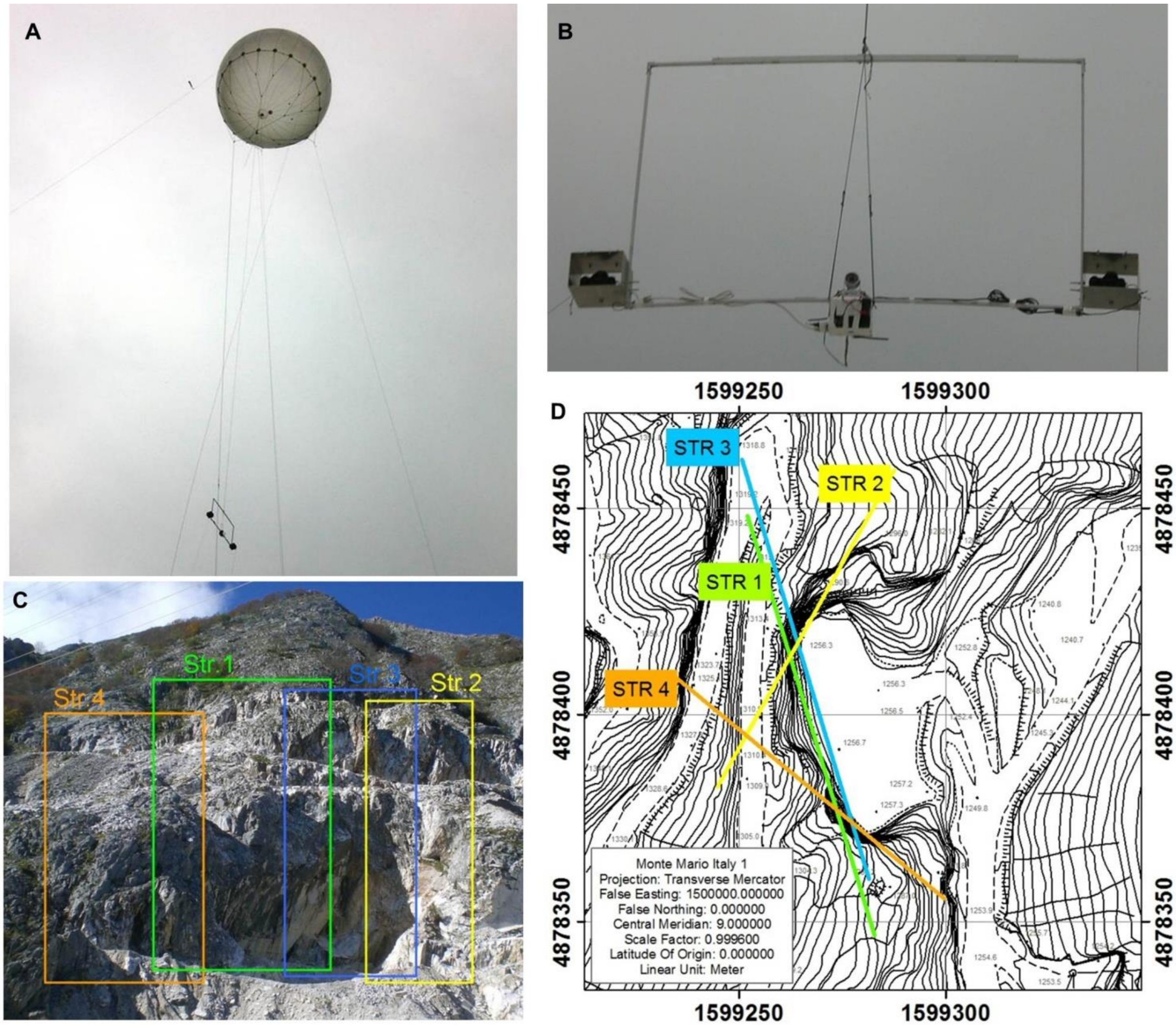

Fig. 2. Photogrammetric survey. A) Aerostatic balloon. B) Photogrammetric aluminium frame with cameras. C) Vertical photogrammetric strips. D) Direction of the aluminium frame during strip acquisition.

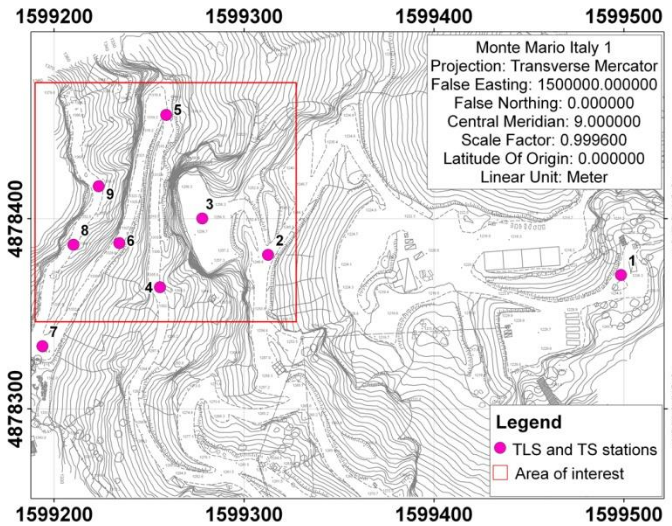

Fig. 3. TLS and TS survey stations.

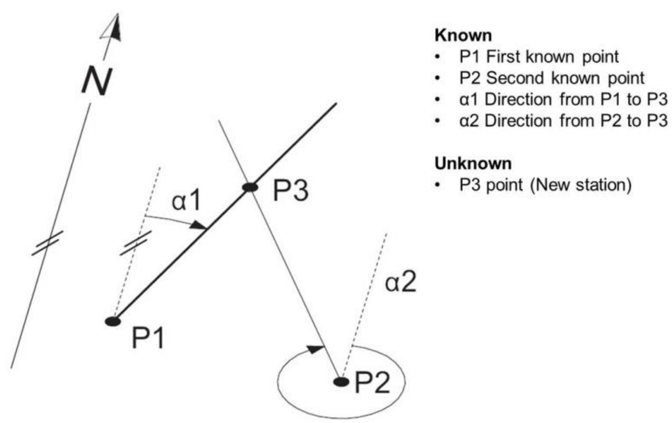

Fig. 4. Intersection Method used to calculate the coordinate of an unknown point (P3) by the acquisition of two known points (P1 and P2 - Image from Leica TPS1200+ Applications Field Manual).

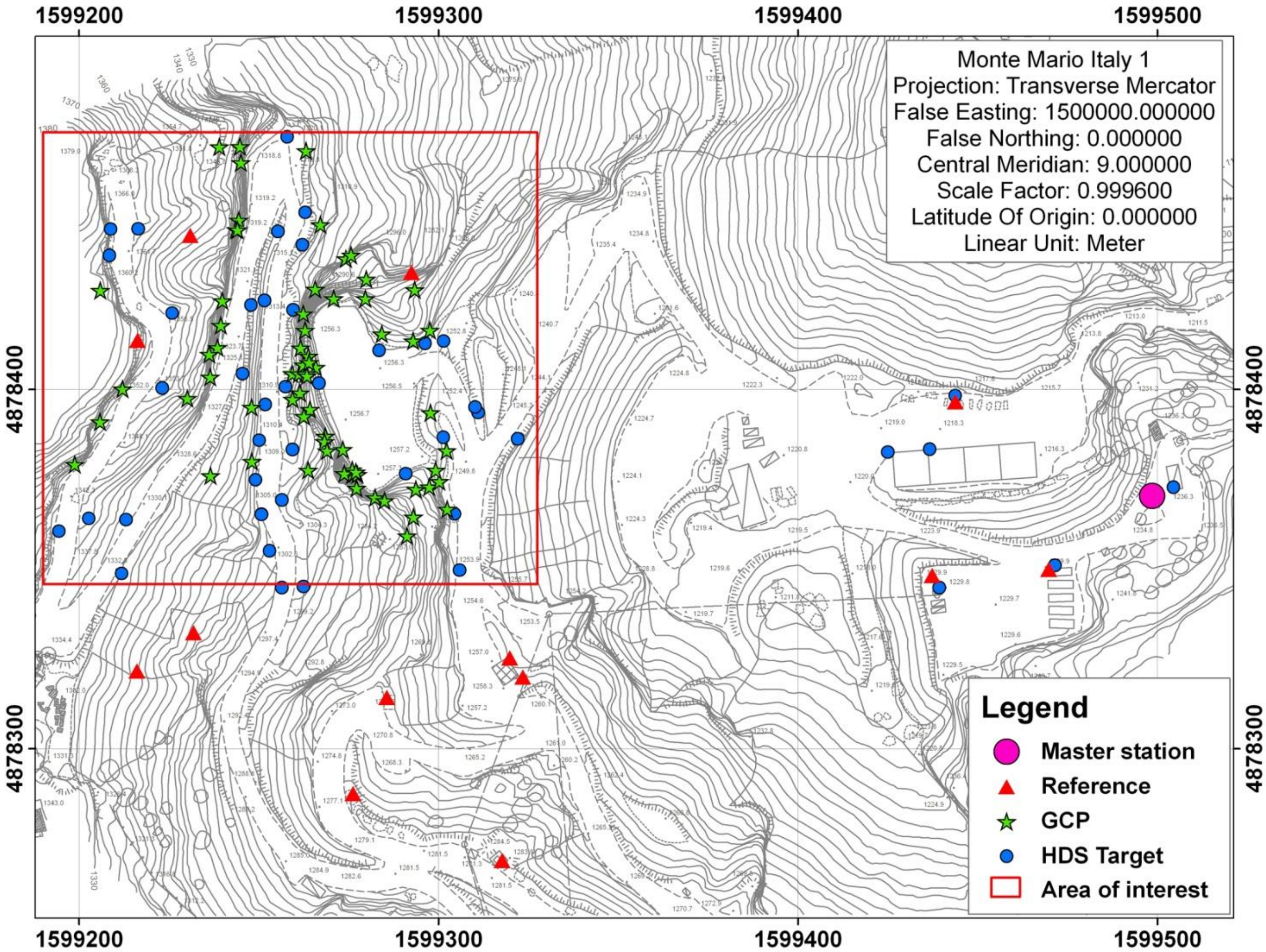

Fig. 5. Map showing points measured with the Total Station and Intersection Method.

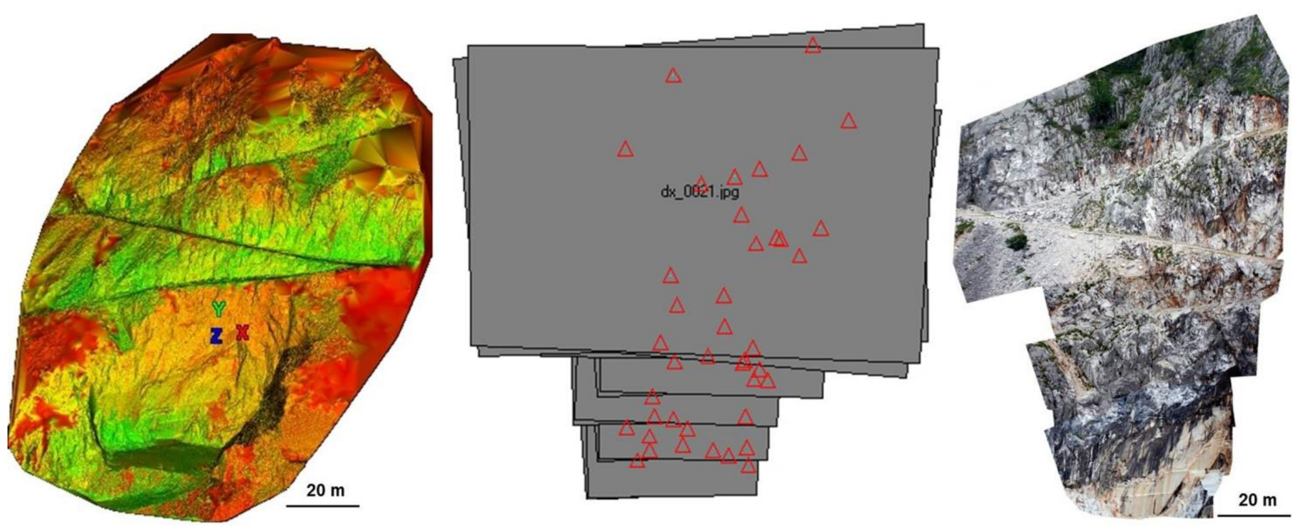

Fig. 6. TLS 3D model (left), photogrammetric block (centre; triangles represent GCPs) and sketch showing high resolution orthophotomosaic (right).

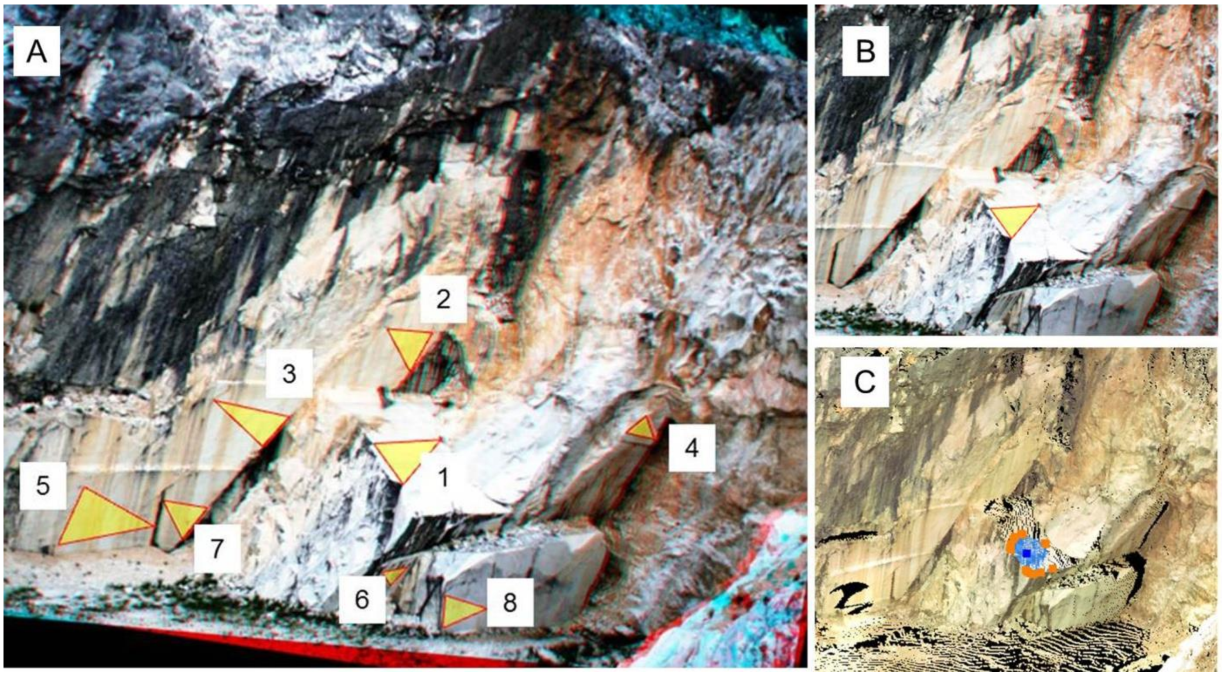

Fig. 7. Measurement of the surface attitudes. A) Stereoscopic model and the surfaces used for the validation process. B) Surface 1 drawn manually on the stereoscopic model. C) Surface 1 extrapolated semi-automatically on the TLS model.

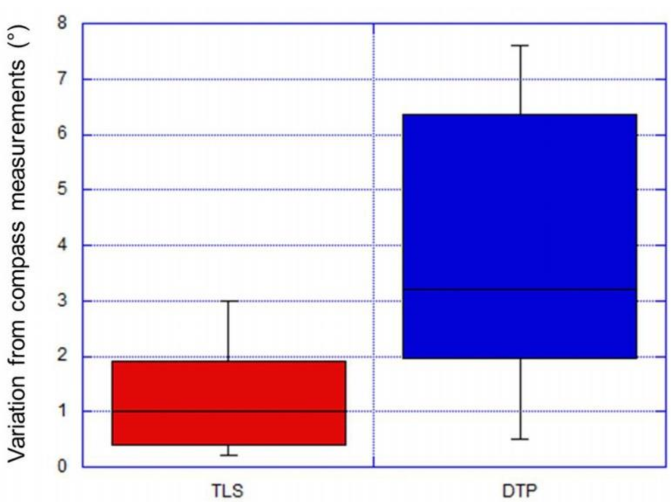

Fig. 8. Box plot representation. Differences between compass and remote sensing measurements (represented in absolute values - degrees).

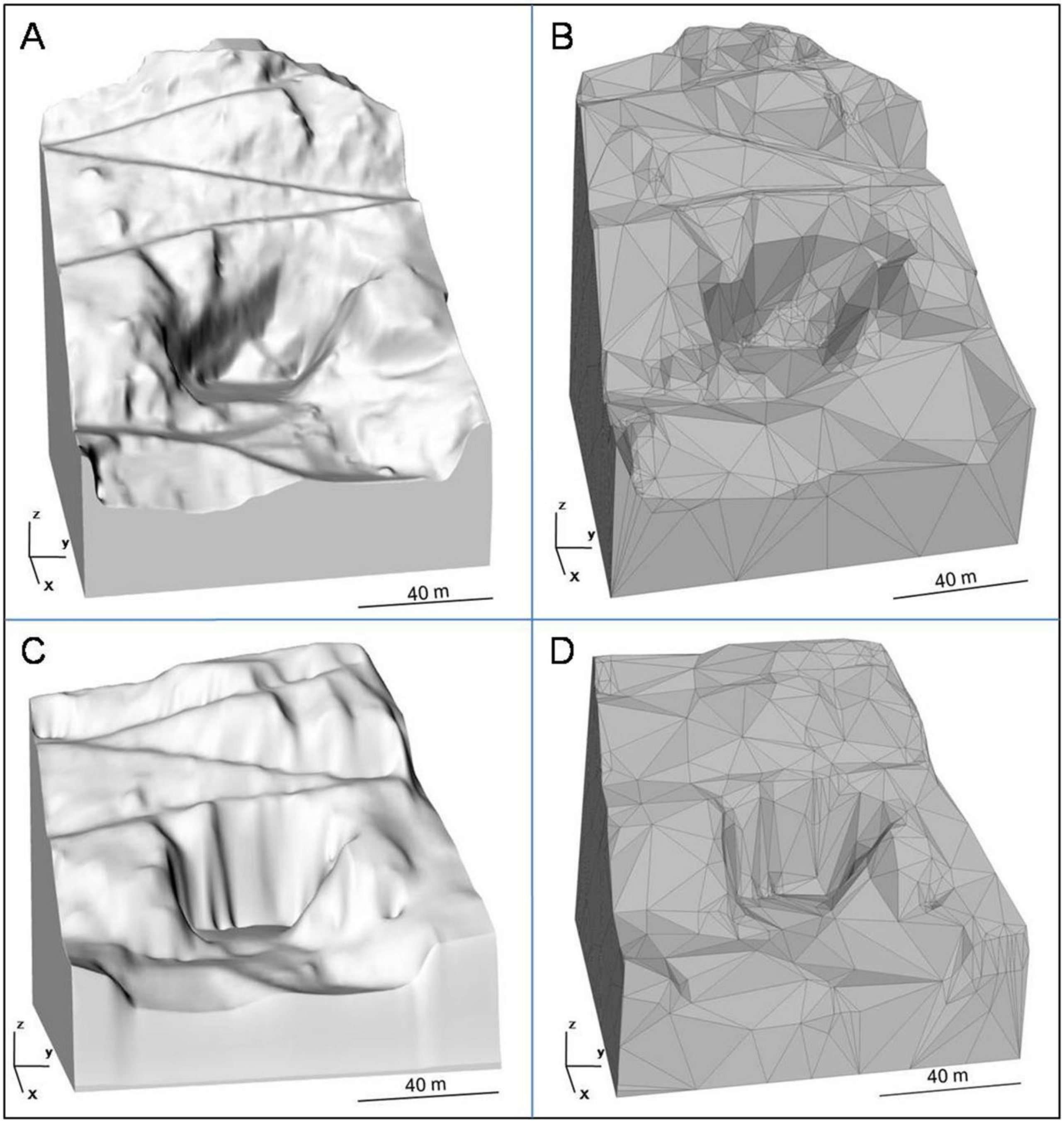

Fig. 9. 3D models of the quarry. TLS model created in Rhinoceros (A) and imported into 3DEC (B). Model from topographic map created in Rhinoceros (C) and imported in 3DEC (D).

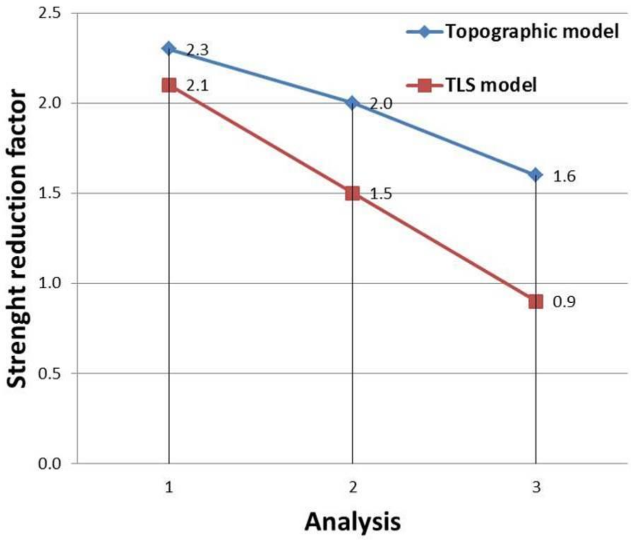

Fig. 10. Change in SRF for the three analyses.

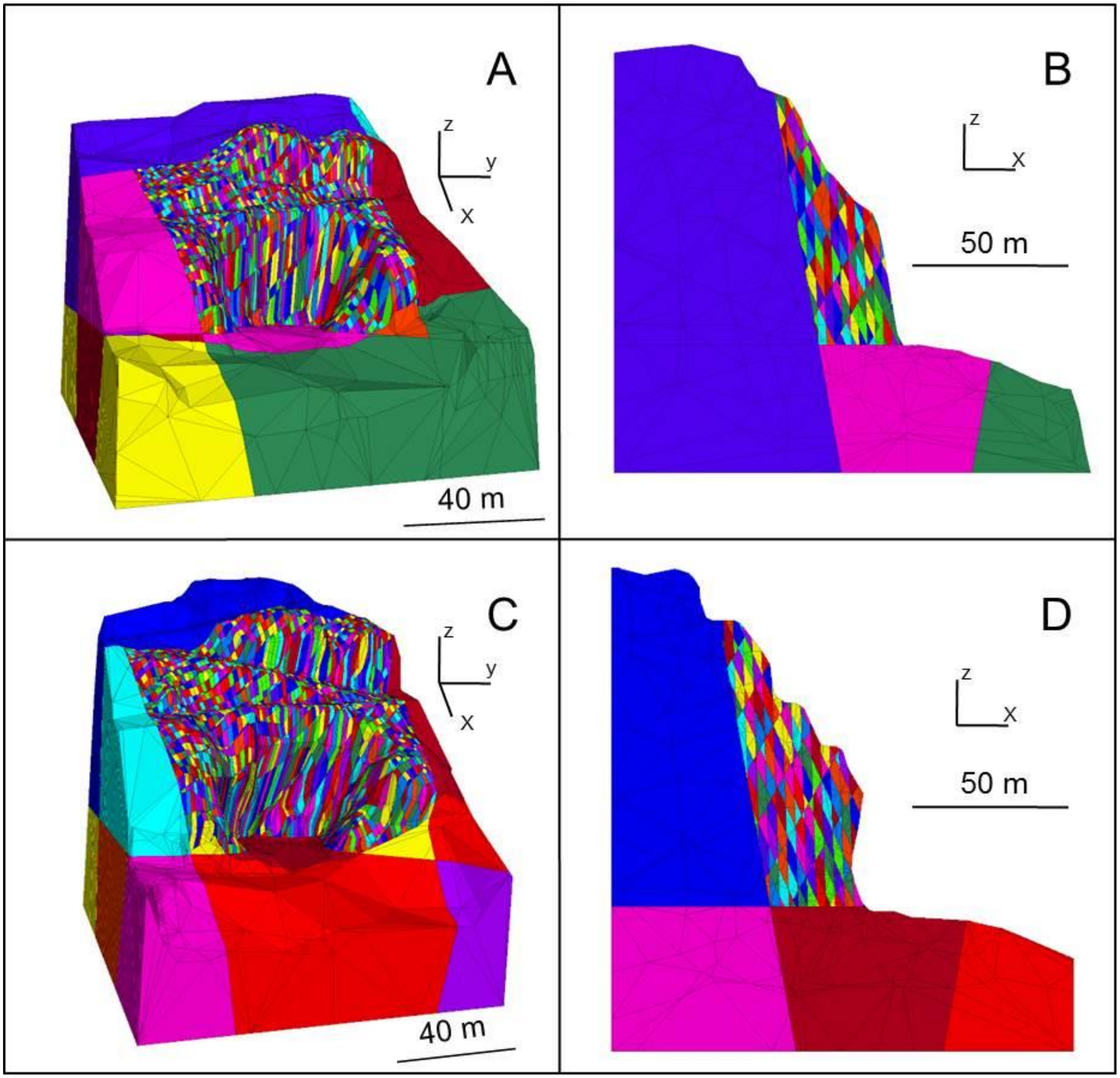

Fig. 11. 3D rock slope models.3DEC model from topographic map (A) and 2D section (B). 3DEC model from TLS (C) and 2D section (D).

Tables

	Image size (Pixel)	Image size (cm)
Width	3872	32.78
Height	2592	21.95

Table 1. Photographic image size

Strip	Lines-of-sight (degrees to North)	RMSE (image unit, pixel)	RMSE (ground unit, cm) areas with highest scale (1:180)	RMSE (ground unit, cm) areas with lowest scale (1:300)
1	260	2.1	3.2	4.9
2	300	3	4.6	7.0
3	260	2.3	3.5	5.3
4	230	4	6.1	9.3

Table 2. Lines-of-sight and image and ground RMSE

	Compass		TLS		DTP	
Surface	Dip Dir	Dip	Dip Dir	Dip	Dip Dir	Dip
1	65	40	65.4	38.1	64.4	36.7
2	240	75	242	73.1	245.9	71.9
3	240	70	240.9	67	243.1	62.4
4	245	70	242.2	69.6	251.9	62.8
5	240	70	239	71.1	238.1	72
6	240	65	240.4	65.2	240.5	58.2
7	240	70	240.3	70.6	245.9	68
8	245	75	244	76	240.4	75.5

Table 3. Dip and dip direction values of rock surfaces measured in the field with a compass, on the TLS point cloud and on the stereoscopic model (DTP).

Joint System	Dip Direction (°)	Dip (°)	Spacing (cm)	Persistence (m)	Aperture (cm)	JRC	JCS (MPa)
K1	157	80	35.9	7.4	0.3	5	37.5
K2	79	88	75.8	3.0	0.2	4	38.3
K3	228	67	262.2	15.7	1.2	13	29.1

Table 4. Characteristics of the main joint systems

Analysis number	Joint Shear Stiffness jks (Pa/m)	Joint Normal Stiffness jkn (Pa/m)	Friction Angle (°)	Cohesion (Pa)	Tensile strength (Pa)	Dilation angle (°)
1	1,00E+09	1,00E+10	30	5,00E+05	5,00E+05	5
2	8,00E+08	8,00E+09	20	4,00E+05	4,00E+05	5
3	6,00E+08	6,00E+09	10	3,00E+05	3,00E+05	5

Table 5. Joint properties used in the 3DEC analyses.

Analysis number	SRF	
	Topographic model	TLS model
1	2.3	2.1
2	2	1.5
3	1.6	0.9

Table 6. SRF achieved from the topographic and TLS models using different joint properties.

Close range Remote sensing	Advantages	Limitations
DTP with aerostatic balloon	Overcomes problems related to elevation, steepness and complex geometry of slope (different lines-of-sight can be used for the survey to avoid problems related to slope orientation). With favourable weather conditions photographs can be acquired with high precision without problems related to the stability of the frame. The high resolution of photographs help in the analysis of slopes.	In practice may be difficult to use Can reach a maximum elevation of 300 m. Not possible to use in case of inaccessibility of the area facing the object under study or unfavourable weather conditions. Expensive compared with the tripod method.
TLS	Easy and fast to use. If integrated with GPS and TLS it is possible perform a “non-static” survey which helps to overcome problems related to point density and slope orientation (different stations with different lines-of-sight can be used for the survey and IM to join all the data in a global reference system). In favourable conditions the output data is extremely precise and representative of the real geometry of the slope.	Not possible to use in case of inaccessibility of the area facing the object under study or unfavourable weather conditions. If the slope is very high occlusion may be present (Sturzenegger and Stead, 2009a). The use of a “static survey” lead to face problem related to point density and slope orientation (Ferrero et al., 2010; Lato et al., 2010)

Table 7. Close range DTP and TLS techniques: advantages and limitations (after Francioni, 2013).

Analysis method	Critical input Parameters (Stead et al., 2006)	Improvement gained from DTP and TLS approach	Limitations
3D Discontinuum modelling (e.g., distinct element, DDA, Lattice-spring)	Slope and discontinuity geometry; intact rock constitutive criteria (elastic, elasto-plastic, etc.); discontinuity stiffness and shear strength; groundwater and in situ stress conditions.	Representative slope geometry is ensured even in case of complex geometry. Major discrete fractures can be identified as well as joint sets (only the rock slope face can be characterized but data for discrete fracture networks can be derived and used to understand the role of brittle fracture, rock bridges and persistence in the analyses; i.e. Sturzenegger 2009b; Tukey et al., 2013).	The data processing and interpretation time when dealing with accurate and detailed data are longer and the model construction is more complex. Only the rock slope face can be characterized. The proposed approach does not provide information about the most suitable constitutive criteria and the joint and rock mass characteristics; nevertheless, some authors (i.e. Fekete et al., 2010; Tatone and Grasselli, 2010) studied the importance of using a 3D approach with high-resolution surface measurements in the definition of these characteristics.

Table 8. Improvements remote sensing techniques offer in the definition of critical input parameters for 3D Discontinuum Codes (after Stead et al., 2006 and Francioni, 2013).